Artificial Pinning Centers and The Quest of High Critical Current Densities in HTS Nanocomposites

Judy Wu, Mohan Panth, Victor Ogunjimi, Bibek Gautam, Jack Shi, Mary Ann Sebastian, Timothy Haugan, Charles Ebbing, Di Zhang, Jie Jian, Jijie Huang, Yifan Zhang, and Haiyan Wang

Abstract— **After theoretical discovery of quantized magnetic vortices in type II superconductors by Abrikosov, which received 2003 Nobel Prize in Physics, vortex pinning has been an important topic of research for high critical current densities in applied magnetic fields desired for a variety of applications in electric and electronic devices and systems. The small vortex core size in high temperature superconductors (HTSs), of a few nanometers, has prompted an intensive research in development of nanoscale artificial pinning centers (APCs) in so-called HTS nanocomposites. Exciting results of much enhanced in-field critical current densities and pinning force densities have been achieved. This talk intends to highlight the progress made recently in HTS nanocomposites towards controllable generation of APCs with desired morphologies, dimension, concentration, and pinning efficiency for targeted applications. The future research in HTS nanocomposites to meet the need of practical applications will also be discussed.**

Index Terms- **HTS nanocomposite film, artificial pinning center, vortex pinning, pinning efficiency, interface engineering**

I. Introduction

After the discovery of the high-temperature superconductivity (HTS) in 1986 by Bednorz and Müller [1], many prototypes of electronic and electric applications based on HTS materials have been explored and demonstrated [2] ranging from lightweight electric propulsion and power generation in aircraft, to more efficient and reliable wind-powered generators, to high efficiency power grid, high-field magnets for accelerators, fusion and medical applications, etc [3]–[9]. HTS materials have high electrical current carrying capability that is quantitatively described by critical current density (J_c) and critical current (I_c), which are regarded as one of most important parameters for practical applications [10], [11]. Therefore, HTS materials can assist reducing energy loss, size and weight, and environment footage of electrical systems. For example, an HTS wind turbine of increased maximum power output by 60% from 5 MW to 8 MW has shown to have reduced weight/volume by about 35% as compared to its counterpart made of copper [9]. However, significant market penetration HTS technologies performance-cost balanced HTS materials. Further enhancement of in-field J_c and I_c, especially HTS $REBa_2Cu_3O_7$ (REBCO, with RE regarding rare earth) coated conductors that employs a strategy of epitaxy of HTS films on flexible metal tapes of textured surface templates, has been the focus of HTS research for large I_c on the order of a few hundreds to thousands Amperes per centimeter width in long length to meet the requirement of power applications [2], [12], 13].

J_c is an intrinsic property of HTS materials but often obstructed by extrinsic factors such as growth defects. Intrinsically, J_c is highly anisotropic in HTS materials due to their layered structures. Higher J_c by orders of magnitude has

[1] This research was supported in part by NSF contracts Nos: NSF-DMR-1909292 and NSF-ECCS-1809293, the AFRL Aerospace Systems Directorate, the Air Force Office of Scientific Research LRIR #14RQO8COR and LRIR #18RQCOR100. (Corresponding author: Judy Wu)

Judy Wu, Mohan Panth, Victor Ogunjimi, and Bibek Gautam are with the Department of Physics and Astronomy, the University of Kansas, Lawrence, Kansas 66045, USA (email: jwu@ku.edu; panthm@ku.edu; victorogunjimi@ku.edu; gautambik@gmail.com)

Mary Ann Sebastian is with the University of Dayton Research Institute Dayton, OH 45469, USA and with the Air Force Research Laboratory, AFRL/RQQM, OH 45433, USA (email: maryann.sebastian@udri.udayton.edu)

Timothy Haugan is with the Air Force Research Laboratory, AFRL/RQQM, OH 45433, USA (email: timothy.haugan@us.af.mil)

Charles Ebbing is with the University of Dayton Research Institute Dayton, OH 45469, USA (email: Charles.Ebbing@udri.udayton.edu)

Di Zhang, Jijie Huang, Yifan Zhang, and Haiyan Wang area with the School of Materials Engineering, Purdue University, West Lafayette, IN 47907, USA (email: zhan2923@purdue.edu; huangjj83@mail.sysu.edu.cn; fantonyzhang@gmail.com; hwang00@purdue.edu)

been observed along the ab-planes than that along the c-axis [14]. This requires HTS films to be c-axis oriented to allow J_c in ab-plane. Furthermore, epitaxy of HTS films is required to eliminate in-plane grain boundaries (GBs) of GB angles in exceeding ~2-3º above which an exponential decrease of J_c with GB angle has been observed due to the d-wave symmetry [15-18]. Reducing the large-angle GBs and hence its limiting effect on J_c has motivated exciting process in the research and development of the coated conductors [13], [19]. High J_c's (77K, SF) in exceeding 1 MA/cm^2 and I_c's > hundreds to thousands Amperes per centimeter width on many kilometers of lengths of coated conductors [2], [12], [13], [19]–[21].

Since most HTS applications require high J_c and I_c in applied magnetic field of a few to tens of Tesla, generating strong pins in HTS, or so-called artificial pinning centers (APCs), becomes critically important and has prompted intensive research during almost the past two decades on APC/REBCO nanocomposites films and coated conductors. Exciting progress has been made. Overall, this research has been driven by many basic questions such as: what impurity materials may form nanoscale APCs through phase segregation in REBCO matrix? Can aligned columnar defect array form along the c-axis of REBCO to address the issue of J_c anisotropy? What controls the APC morphology, dimension, and orientation? Do all formed APCs contribute to pinning and what is the upper limit of their pinning efficiency? This paper intends to highlight the efforts and achievements in answering these questions through understanding the growth mechanism of APC/REBCO nanocomposites, using which to control the microstructures of APCs in APC/REBCO nanocomposites for desired pinning landscape, and their impact on J_c.

II. Result and Discussion

A. *Artificial Pinning Centers (APCs)*

Various APCs of different morphologies, including c-axis aligned one-dimensional nanorods (1D-APCs), ab-plane aligned two-dimensional planar defects (2D-APCs), and three-dimensional nanoparticles (3D-APCs) have been reported (Fig. 1) through the addition of impurity dopants such as $BaZrO_3$ (BZO), $BaHfO_3$ (BHO), $BaSnO_3$ (BSO), $YBa_2(Nb/Ta)O_6$, Y_2O_3, etc. in REBCO (RE=rare-earth elements: Y, Er, Gd, Nd, Sm) and enhanced pinning has been achieved in these APC/REBCO nanocomposite films [11], [13], [19]–[47]. Among others, BZO-1D APCs have been comprehensively studied after the first report by MacManus-Driscoll *et al* [48] since they can form as c-axis aligned arrays in a broad range of BZO doping concentration with areal density proportional approximately linearly to the BZO doping, which is important to obtain optimal pinning in applications targeted at specific magnetic fields.

B. *Critical Role of Strain Field on APC Self-organization*

In physical vapor deposition (such as magnetron sputtering and pulsed laser deposition) and chemical vapor deposition, epitaxial APC/REBCO nanocomposite films grow in the layer-by-layer mode. Since the sources of APC and REBCO are

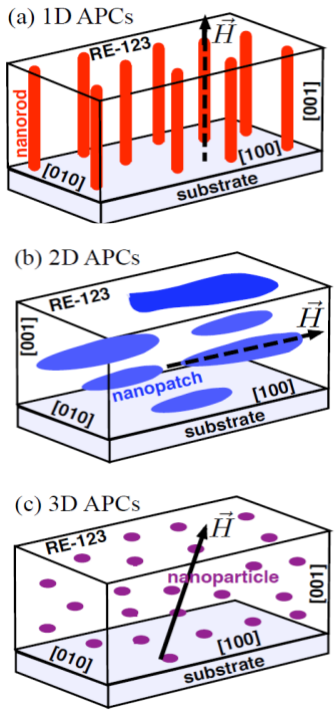

Fig. 1. Schematic definition of (a) 1D, (b) 2D, and (c) 3D APCs. Reproduced with permission from *Wu and Shi* 2017 Supercond. Sci. Technol. 30 103002. Copyright 2017 Institute of Physics, United Kingdom

coated together, APCs form through phase segregation from the REBCO matrix at the initial stage of the growth, which is affected by the growth condition, lattice mismatch at interfaces and elastic properties of the APC and HTS materials. For APC/REBCO nanocomposite films, there are three coherent or semi-coherent (with defects) interfaces including APC/REBCO, APC/substrate and REBCO/substrate interfaces as shown schematically in Fig. 2. Strains arise because of the lattice mismatches at these interfaces serve as the driving force for the phase segregation, or so-called strain-mediated self-organization, and hence nucleation and evolution of APCs through the film thickness. The strain field is accommodated through lattice expansion and compression in the

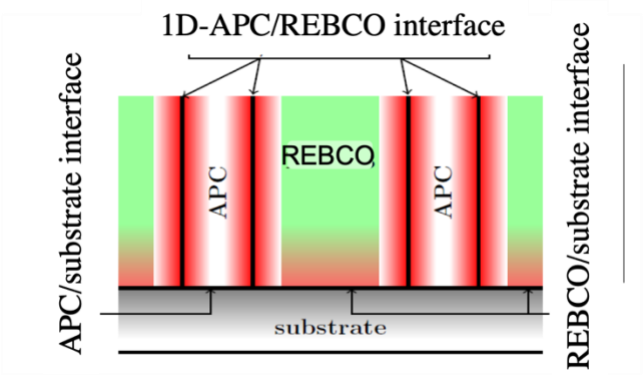

Fig. 2. Strain field initiated from the strained interfaces plays a critical role in strain-mediated APC self-organization. Reproduced with permission from *Wu and Shi* 2017 Supercond. Sci. Technol. 30 103002. Copyright 2017 Institute of Physics, United Kingdom

nanocomposite and therefore complicated by the different elastic properties of REBCO, APC and substrate materials. The accommodation is the least in the substrate since its thickness is larger by many orders of magnitude than dimension of APC and REBCO film thickness. Therefore, the contribution of the substrate elastic property is often neglected assuming only REBCO and APCs will accommodate to the strain field generated. In both APC and REBCO, the strain may extend from the interfaces and the extension depends on their elastic properties typically in the range of a few to tens of nanometers. This leads to a highly non-uniform strain field in the APC/REBCO nanocomposite films. Interestingly, the reported APCs have different morphologies of 1D, 2D and 3D, different dimensions and orientations. While often the lattice mismatch between APC and REBCO is the first consideration in APC material selection, how it affects the APC morphology, dimension and orientation quantitatively requires a systematic study. In addition, the role of the elasticity of the two involved lattices should also be considered. To shed lights on this, an APC/REBCO nanocomposite film was investigated in an elastic strain model with consideration of the elastic constants and the lattice mismatches at three interfaces shown in Fig. 2 including the REBCO/substrate interface, the 1D APC/REBCO interface the 1D APC/substrate interface [49]. By minimizing the elastic energy, a few interesting insights have been obtained.

C. Effects of strain field on APC morphology, dimension and orientation

The first question to answer in the elastic strain model simulation is why some impurity materials would form 1D APCs while others are not. Fig. 3a depicts an APC morphology phase boundary (solid line) calculated as function of the ratio absolute value of f_1/f_3 of the lattice mismatches f_1 and f_3 between YBCO matrix and APC dopant in ab-plane and c-axis, respectively, and the elastic constants of the APC (C_{ij}, i, j=1, 2, 3) [49]. The simulation has revealed a phase boundary (solid line) between c-axis aligned 1D APCs preferred energetically above the line and not preferred below the line by considering both lattice mismatch and elastic properties of the APC and REBCO matrix. Also included in Fig. 3a are experimentally confirmed c-axis aligned 1D APCs (red) of BZO [33]–[35] BSO [39], BHO [31], [32], [50] and YBa_2NbO_6 (YBNO) [29], [30] and CeO_2 and Y_2O_3 3D APCs [36], [51], [52]. It should be noted that some 3D APC impurity materials such as Y_2O_3 may form nanocolumns possibly due to special growth conditions [53]. The agreement between experiment and theory confirms the critical role of the strain field initiated in nucleation, phase segregation and diffusion of the APCs in the REBCO matrix and hence the resulting APC morphology. Also included in Fig. 3a are four simulation predicted 1D APC materials of $CaHfO_3$, $SrHfO_3$, $CaSnO_3$ and $SrZrO_3$ (blue) using their reported elastic constants [54]–[56]. Confirmation of these 1D APCs experimentally would be important to further application of the simulation for APC material prediction.

Fig. 3b depicts the calculated diameter range of the 1D APCs as function of the APC strain decay constant $\lambda_1(2)$ with the ratio of C_{11}/C_{13} of the APC material selected in the range of 1.5-1.1 for a comparison with experiment [57]. It also includes a few examples of 1D APCs demonstrated experimentally (red). Interestingly, the diameters of these 1D APCs agree well with that from the simulation. In addition, the simulation predicts the four possible 1D APC materials of $CaHfO_3$, $SrHfO_3$, $CaSnO_3$ and $SrZrO_3$ (blue) may have smaller diameters, which is desirable for enhanced pinning especially at low temperatures to be comparable to the coherence length of REBCO.

An additional question is on the correlation of the strain field and the orientation of the APC. In order to answer the question, an APC orientation phase diagram was calculated using the elastic strain energy model with consideration of the REBCO/substrate lattice mismatch and strain field overlap at variable APC concentrations [58]. The solid line in Fig. 3c is the calculated phase boundary [59], [60] of the BZO APC orientation in YBCO matrix as a function of BZO APC volume concentration in the nanocomposite film (ρ_{film}) estimated from

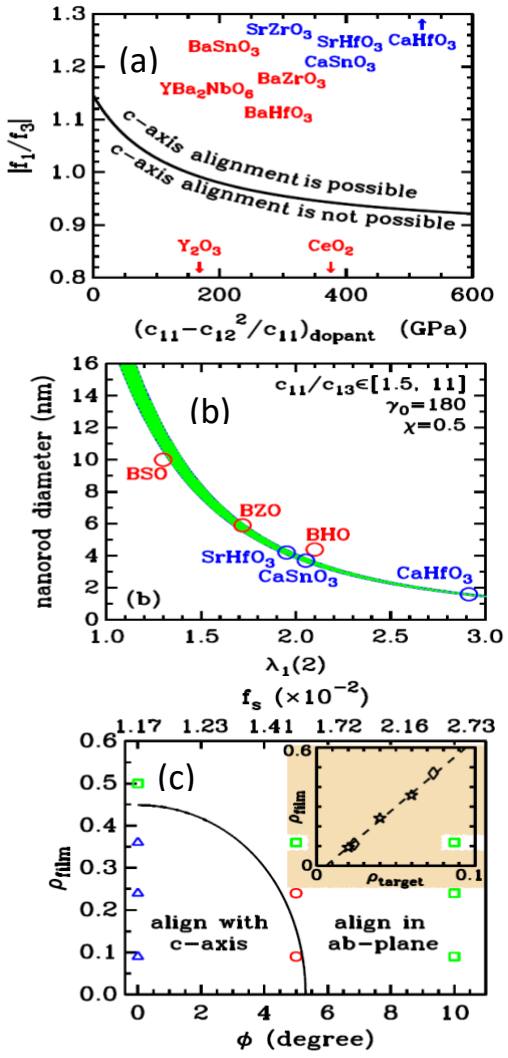

Fig. 3. Simulation results from the elastic strain energy model on (a) morphology of APCs, (b) diameter of 1D-APCs, and (c) orientation of APCs. Solid lines are simulation results and symbols are from experiments. Reproduced with permission from *Wu and Shi* 2017 Supercond. Sci. Technol. 30 103002. Copyright 2017 Institute of Physics, United Kingdom

the transmission electron microscopy (TEM) and the YBCO/substrate lattice mismatch f_s in the range of 1.2 to 2.7% (top scale). In this positive f_s range, the REBCO matrix is subjected to a tensile strain in the ab-plane or a compressive strain along the c-axis. The positive f_s can be obtained using $SrTiO_3$ vicinal substrates (Φ is the vicinal angle). By increasing the vicinal angle Φ, the ab-plane tensile strain can be quantitatively tuned from low to high. Therefore, at the lower ab-plane tensile strain and lower ρ_{film} (inside the phase boundary), the c-axis alignment remains energetically preferred for 1D APCs. Beyond this region at larger vicinal angle Φ and higher ρ_{film}, the ab-aligned APC become energetically favorable. The symbols in Fig. 3c are experimental data [61]–[63]. The simulation result agrees well with experiment. In particular, mixed c-axis and ab-plane oriented APCs could co-exist, which has been observed experimentally (red symbols) [62].

D. Effects of growth condition on APC nucleation and evolution

It should be noted that the formation of APCs is critically affected by the processing conditions such as growth temperatures. Figs. 4a-f displays the cross-sectional TEM images of BZO 1D APCs grown in YBCO films at different temperatures (T_g) in the range 780-835 °C [64]. At lower temperatures, only sparse, short segmented 1D APCs are visible. At higher temperatures, both the length (green symbols in Fig. 4g) and the concentration of the 1D APCs are significantly increased. Note the six films were made from the same PLD target at fixed BZO doping, suggesting the phase segregation of BZO in YBCO requires adequate energy. Without such an energy, BZO may remain on the YBCO lattice as chemical doping. Furthermore, the phase segregation may be hindered by the presence of other APCs such as Y_2O_3 3D APCs as shown in Fig. 4g (blue) [65] since the strain field is disturbed locally considerably.

When the modulated strain field is disturbed, the strain mediated self-assembly of BZO 1D APC arrays aligned perfectly along the c-axis of REBCO may no longer be energetically favorable. This means that a mixed APC landscape could be generated through engineering the strain field by introduction of a secondary APC impurity such as Y_2O_3. While Y_2O_3 may often form 3D APCs, the BZO (or other 1D APC materials) may form APCs of different morphologies. Fig. 5a shows schematically a pinning landscape that combines 1D, 2D and 3D APCs. The mixed APC morphology may provide favorable pinning landscape to reduce the anisotropy of J_c with respect to the magnetic field orientation variations. Fig. 5b exhibits a cross-sectional TEM image of a 4 vol.% BHO+3 vol.% Y_2O_3 doped YBCO film that contains BHO 1D APC (red arrows), 2D APC (blue arrows) and 3D APCs (most probably Y_2O_3 and possibly BHO as well) [66]. An immediate benefit of the mixed pinning landscape is in the reduced anisotropy of J_c at different orientations of magnetic field or different angle θ that is defined as the angle between

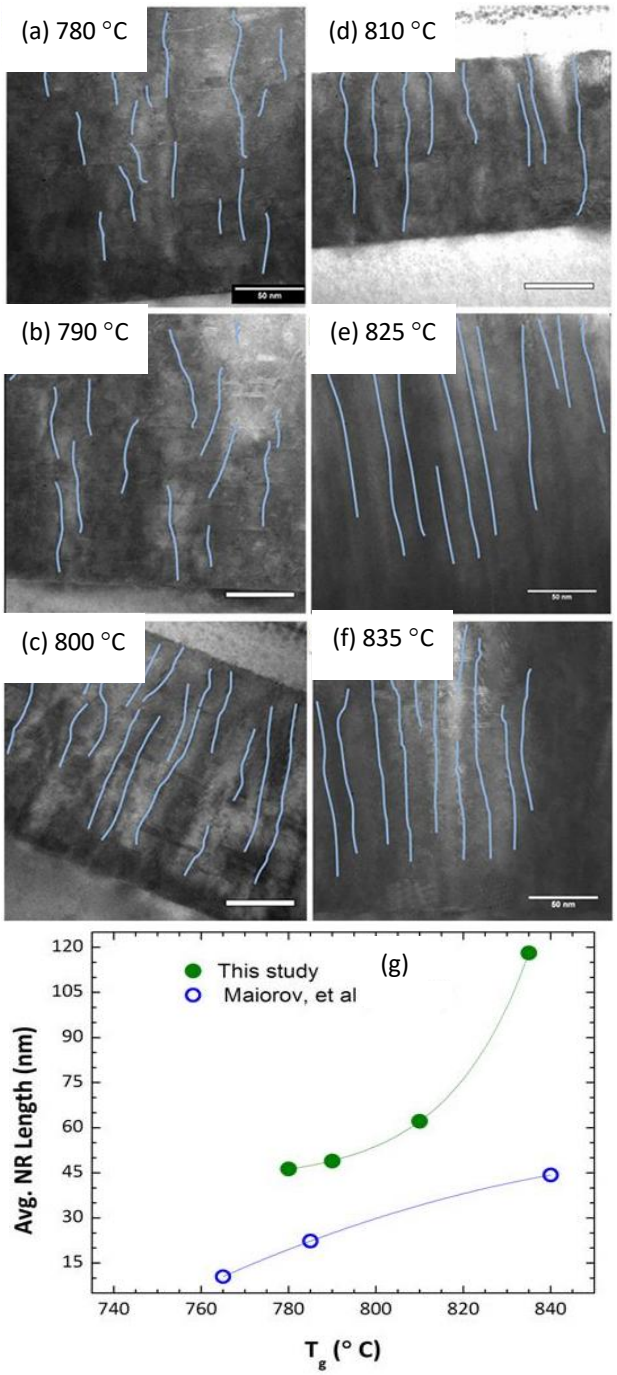

Fig. 4. (a-f) Cross-sectional STEM image BZO/YBCO nanocomposite films grown at different temperatures in the range of T_g ~780-835 °C (g) BZO 1D APC length as a function of T_g in BZO/YBCO without (green) and with (blue) Y_2O_3 nanoparticles

the magnetic field and the c-axis of YBCO. Fig. 5c shows the $J_c(\theta)$ curves measured at 65 K and 1 T, 5 T, and 9 T on 2 (red), 4 (black), 6 (blue) vol. % BHO+3 vol.% Y_2O_3/YBCO nanocomposite films. High and less anisotropic J_c has been observed on the samples with mixed APCs. Among the three samples, the best result is observed on the 4 vol.% BHO+3 vol.% Y_2O_3 doped YBCO, indicating the importance in balancing the APCs of difference morphologies.

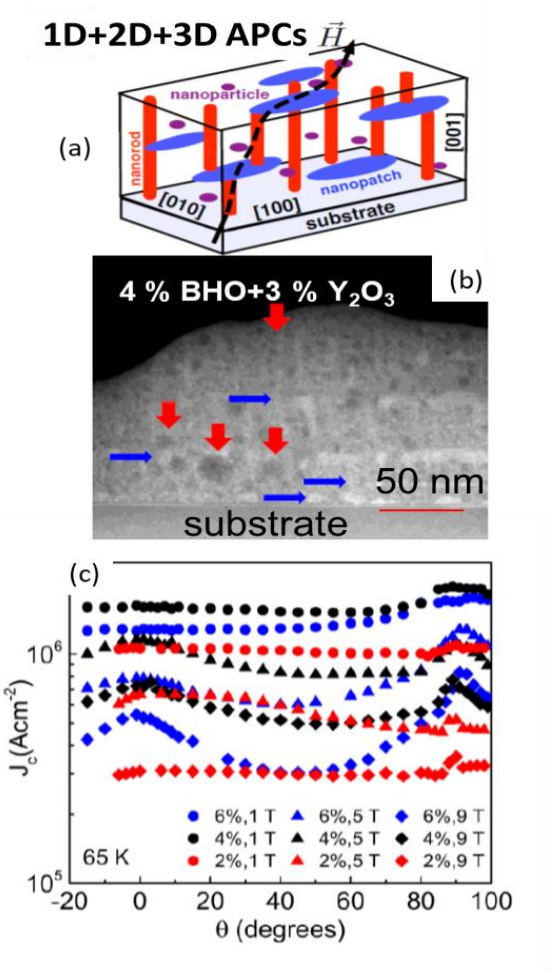

Fig. 5. (a) schematic of a mixed pinning landscape of 1D, 2D and 3D APCs. (b) Cross-sectional view of TEM on a 4 vol. % BHO+3 vol.% Y_2O_3/YBCO nanocomposite film containing 1D (red), 2D (blue) and 3D APCs. $J_c(\theta)$ measured on 2 (red), 4 (black), 6 (blue) vol. % BHO+3 vol.% Y_2O_3/YBCO films at 65 K.

E. Impact of APC/REBCO strained interface on $J_c(H)$

While strain field plays a critical role in nucleation and evolution of APCs and hence provides the control on the APC morphology, dimension and orientation, the strain initiated from the large lattice mismatch at APC/REBCO interface may lead to formation of defects when the strain is too high to bear by the APC and REBCO lattices. Consequently, a defective APC/REBCO interface APC/REBCO interface forms and leads to degradation of superconducting properties of the BZO/YBCO nanocomposites especially reduced pinning efficiency of the 1D APCs [67]-[69]. In a comparative study on BZO/YBCO (with lattice mismatch of ~7.7%) and BHO/YBCO (with lattice mismatch of ~6.9%) nanocomposite films, a semi-coherent APC/YBCO interface in the former is blamed for the much lower pinning efficiency of BZO 1D APCs than that their counterpart BHO 1D APCs which form a more coherent interface with YBCO [70]. Since the specific pinning force (or pinning force per unit length) of the 1D APCs is proportional to the radial derivative of the pinning energy at the 1D APC/YBCO interface [71], a coherent interface without degradation of superconductivity is desired for optimal pining. This result raises a question whether a general approach could be developed to obtain a coherent 1D APC/REBCO interface for high pinning efficiency.

In order to answer this question, we have developed a multilayer (ML) scheme to dynamically enlarge the c-lattice constant of YBCO after or during the BZO 1D-APC formation through Ca doping into the tensile strained BZO/YBCO interface [72]. As shown schematically in Fig. 6a, the bottom BZO/YBCO layer (Step 1) of thickness in the range of tens to hundreds of nm is identical to the case of single layer (SL) BZO/YBCO

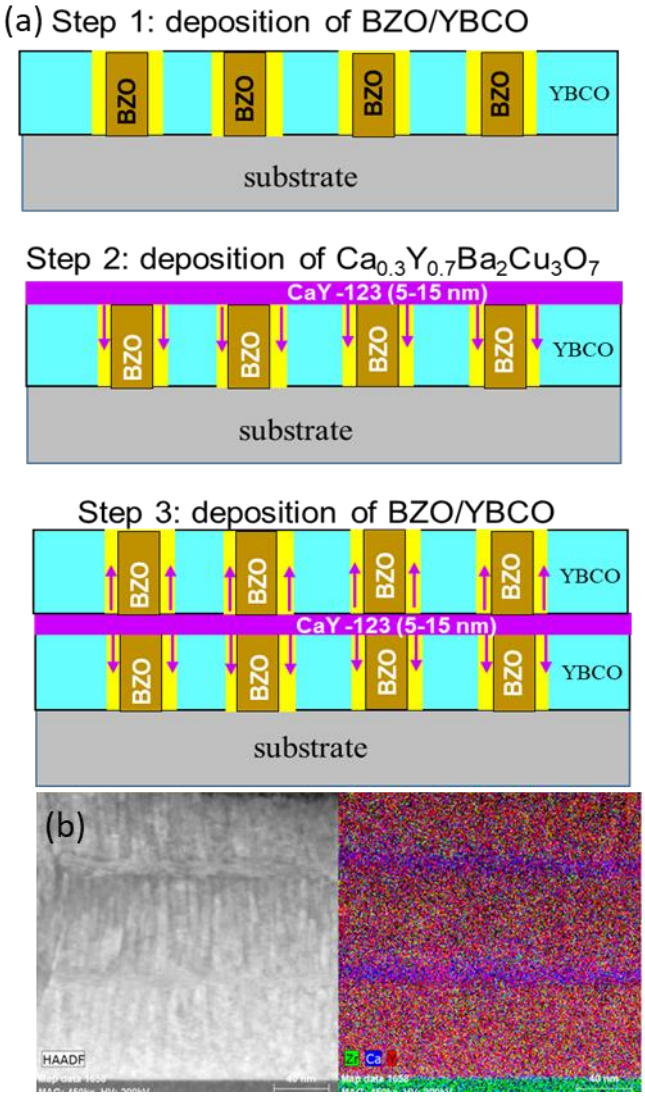

Fig. 6. (a) Schematic illustration of the ML approach and (b) cross-sectional TEM and EDX map on a 6 vol% BZO/YBCO ML sample.

nanocomposite films. This means the BZO 1D APCs would have the same morphology and concentration in this layer. Step 2 is for deposition of a thin (5-15 nm thick) $Ca_{0.3}Y_{0.7}Ba_2Cu_3O_{7-x}$ (CaY123) spacer layer on the BZO/YBCO nanocomposite film to allow Ca diffusion during the in-situ film growth. These two steps can be repeated for thicker samples. The tensile strained BZO/YBCO interface has been found to provide a diffusion channel for Ca, yielding Ca/Cu substitution on the Cu-

O planes of YBCO near the interface. Since Ca ion is 30% larger than Cu ion, this leads to enlarged c-lattice constant up to 1.24 nm and hence reduced BZO/YBCO lattice mismatch from 7.7% to 1.4% as confirmed in a TEM study [73]. This prevents formation of defects at the BZO/YBCO interface and leads to enhanced J_c in magnetic fields up to 9 T at H//c-axis and other orientations [73]–[76]. It should be noted that Ca/Y and Ca/Ba substitutions are also possible on YBCO lattice. Without any strain, Ca+2/Y+3 substitution would be the most favored energetically considering the smallest difference of ~11% in the ionic radii of Ca+2 and Y+3, which is consistent to the reported Ca/Y substitution in YBCO for the overdoping effect due to the valance difference in Ca+2 and Y+3 [77].

Fig. 7 compares the J_c(H) curves measured at different temperatures of 65 K and 77 K respectively on a pair of 6 vol.% BZO/YBCO ML (solid) and SL (open) samples. At 77 K, the former shows higher J_c(H) at higher H fields. At 65 K, the ML sample has significantly higher J_c(H) over the entire field range of 0-9.0 T. Specifically at 9 T, the J_c in the ML film is about five times of that of the SL counterpart. This result sheds light on the importance controlling the APC/REBCO interface and demonstrates the ML approach provides a promising scheme to improve the interface and the pinning efficiency of BZO 1DAPCs.

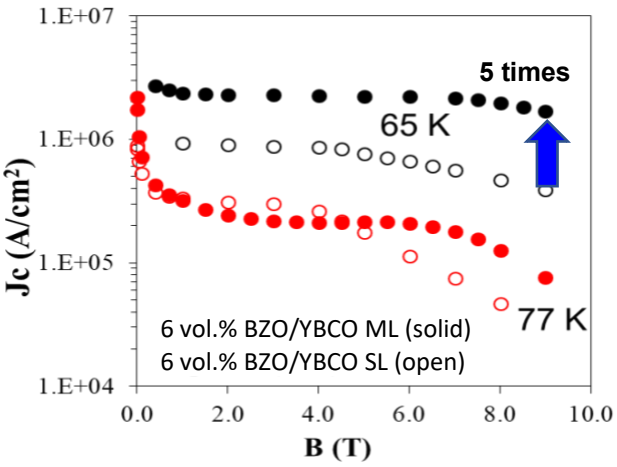

Fig. 7. J_c(H) curves measured on 6 vol.% BZO/YBCO ML (solid) and SL (open) film respectively at H//c-axis.

III. Conclusions

In summary, significant progress has been made in the last two decades in research and development of APCs in REBCO films and coated conductors. Various APCs with different morphologies of 1D, 2D and 3D, together with pinning landscapes of APCs of mixed morphologies have been reported with improved pinning and hence enhanced J_c(H). At a more fundamental level, a good understanding of the growth mechanism of the APCs in the APC/REBCO nanocomposites films has been achieved using the elastic-strain energy modeling and simulation. In particular, the effect of the strain field initiated from the mismatched interfaces on the APC morphology, dimension and orientation has been evaluated and the understanding has allowed interpretation of the experimental observations as well as prediction of APC microstructures. More recently, the effect of APC/REBCO interface on the specific pinning efficiency of 1D APCs has been investigated, revealing the formed APCs may not contribute to pinning or to the full strength due to the defective interface. This has motivated new schemes to be developed for engineering the APC/REBCO interface. Among others, the ML scheme was shown effective to reduce the interface strain by dynamically enlarging the c-axis of YBCO and hence reduding the BZO/YBCO lattice mismatch from 7.7% to 1.4% near the interface. The resulted coherent BZO/YBCO interface justifies well the much enhanced J_c(H) by up to five folds at 65 K and 9 T in ML samples as compared to the SL counterparts. This result suggests further enhancement of J_c(H) and the peak field of pinning force density approaching the accommodation field defined from the APC concentration could be achieved with a thorough understanding of the interface effect and new interface engineering schemes to be developed. Besides temperatures near T_c, further extension of the benefit of enhanced pinning to lower temperatures would be important and requires a systematic investigation. Furthermore, a more interactive approach between pinning landscape simulation based on requirement of specific applications and controllable APC growth would be necessary in future research. Finally, besides consideration of pinning, other properties, such as mechanical strength and thermal conduction, may be implemented to APC/REBCO nanocomposites to address the need for high J_c(H), high mechanical strength, thermal uniformity, etc. for practical applications.

References

[1] J. G. Bednorz and K. A. Muller, "Possible High-Tc Superconductivity in the Ba-La-Cu-O System," (in English), *Zeitschrift Fur Physik B-Condensed Matter,* vol. 64, no. 2, pp. 189-193, 1986. [Online]. Available: <Go to ISI>://A1986D856200010.

[2] "DOE Workshop Report on Basica Research Needs for Superconductivity," *www.sc.doe.gov/bes/reports/abstracts.html#sc,* 2005.

[3] X. Obradors and T. Puig, "Coated conductors for power applications: materials challenges," *Superconductor Science and Technology,* vol. 27, no. 4, p. 044003, 2014.

[4] D. Uglietti, "A review of commercial high temperature superconducting materials for large magnets: from wires and tapes to cables and conductors," *Superconductor Science and Technology,* vol. 32, no. 5, p. 053001, 2019.

[5] J. L. MacManus-Driscoll and S. C. Wimbush, "Processing and application of high-temperature superconducting coated conductors," *Nature Reviews Materials,* vol. 6, no. 7, pp. 587-604, 2021.

[6] C. A. Luongo *et al.*, "Next Generation More-Electric Aircraft: A Potential Application for HTS Superconductors," (in English), *Ieee Transactions on*

Applied Superconductivity, vol. 19, no. 3, pp. 1055-1068, Jun 2009, doi: Doi 10.1109/Tasc.2009.2019021.

[7] R. L. Holtz *et al.*, "High Temperature Superconductors for Naval Power Applications," *Materials Science and Technology: 2006 NRL Review,* pp. 1-3, 2006.

[8] P. N. Barnes, M. D. Sumption, and G. L. Rhoads, "Review of high power density superconducting generators: Present state and prospects for incorporating YBCO windings," (in English), *Cryogenics,* vol. 45, no. 10-11, pp. 670-686, Oct-Nov 2005, doi: DOI 10.1016/j.cryogenics.2005.09.001.

[9] J. N. A. Matthews, "Superconductors to boost wind power," (in English), *Physics Today,* vol. 62, no. 4, pp. 25-26, Apr 2009. [Online]. Available: <Go to ISI>://WOS:000264991800014.

[10] A. P. Malozemoff, "High T-c for the power grid," (in English), *Nature Materials,* vol. 6, no. 9, pp. 617-619, Sep 2007. [Online]. Available: <Go to ISI>://000249236200002.

[11] S. R. Foltyn *et al.*, "Materials science challenges for high-temperature superconducting wire," (in English), *Nature Materials,* vol. 6, no. 9, pp. 631-642, Sep 2007. [Online]. Available: <Go to ISI>://000249236200014.

[12] M. P. Paranthaman and T. Izumi, "High-performance YBCO-coated superconductor wires," (in English), *Mrs Bulletin,* vol. 29, no. 8, pp. 533-536, Aug 2004. [Online]. Available: <Go to ISI>://000223315300007.

[13] D. Larbalestier, A. Gurevich, D. M. Feldmann, and A. Polyanskii, "High-T-c superconducting materials for electric power applications," (in English), *Nature,* vol. 414, no. 6861, pp. 368-377, Nov 15 2001. [Online]. Available: <Go to ISI>://000172150700057.

[14] J. Z. Wu and W. K. Chu, "Anisotropy of the transport critical current in (110)-, (113)-, and a-axis-oriented YBa2Cu3O7 thin films," *Phys Rev B,* vol. 49, no. 2, pp. 1381-1386, 01/01/ 1994, doi: 10.1103/PhysRevB.49.1381.

[15] D. Dimos, P. Chaudhari, and J. Mannhart, "Superconducting Transport-Properties of Grain-Boundaries in YBa2Cu3O7 Bicrystals," (in English), *Phys Rev B,* vol. 41, no. 7, pp. 4038-4049, Mar 1 1990. [Online]. Available: <Go to ISI>://A1990CU14000017.

[16] A. Schmehl *et al.*, "Doping-induced enhancement of the critical currents of grain boundaries in YBa2Cu3O7-delta," (in English), *Europhysics Letters,* vol. 47, no. 1, pp. 110-115, Jul 1 1999. [Online]. Available: <Go to ISI>://000081559800018.

[17] G. Hammerl *et al.*, "Enhanced supercurrent density in polycrystalline YBa2Cu3O7-delta at 77 K from calcium doping of grain boundaries," (in English), *Nature,* vol. 407, no. 6801, pp. 162-164, Sep 14 2000. [Online]. Available: <Go to ISI>://WOS:000089241000040.

[18] X. Y. Song, G. Daniels, D. M. Feldmann, A. Gurevich, and D. Larbalestier, "Electromagnetic, atomic structure and chemistry changes induced by Ca-doping of low-angle YBa2Cu3O7-delta grain boundaries," (in English), *Nature Materials,* vol. 4, no. 6, pp. 470-475, Jun 2005. [Online]. Available: <Go to ISI>://000229502700014.

[19] A. Goyal, *Second-generation HTS conductors*. Springer, 2005.

[20] X. Obradors and T. Puig, "Coated conductors for power applications: materials challenges," *Superconductor Science and Technology,* 2014, doi: 10.1088/0953-2048/27/4/044003.

[21] K. Matsumoto and P. Mele, "Artificial pinning center technology to enhance vortex pinning in YBCO coated conductors," *Superconductor Science and Technology,* vol. 23, no. 1, p. 014001, 2009.

[22] P. Mele *et al.*, "Ultra-high flux pinning properties of BaMO3-doped YBa2Cu3O7− x thin films (M= Zr, Sn)," *Superconductor Science and Technology,* vol. 21, no. 3, p. 032002, 2008.

[23] J. Wu and J. Shi, "Interactive modeling-synthesis-characterization approach towards controllable in situ self-assembly of artificial pinning centers in RE-123 films," *Superconductor Science and Technology,* vol. 30, no. 10, p. 103002, 2017.

[24] S. Miura *et al.*, "Strongly enhanced irreversibility field and flux pinning force density in SmBa2Cu3Oy-coated conductors with well-aligned BaHfO3 nanorods," *Applied Physics Express,* vol. 10, no. 10, p. 103101, 2017.

[25] S. Chen *et al.*, "Generating mixed morphology BaZrO3 artificial pinning centers for strong and isotropic pinning in BaZrO3–Y2O3 double-doped YBCO thin films," *Superconductor Science and Technology,* vol. 30, no. 12, p. 125011, 2017.

[26] S. Chen *et al.*, "Enhancement of isotropic pinning force in YBCO films with BaZrO3 nanorods and Y2O 3 nanoparticles," *IEEE Transactions on Applied Superconductivity,* vol. 27, no. 4, pp. 1-5, 2016.

[27] E. Galstyan, R. Pratap, M. Paidpilli, G. Majkic, and V. Selvamanickam, "Pinning Characteristics of Zr and Hf-Added REBCO Coated Conductors Made by Advanced MOCVD in Low-to-High Magnetic Fields," *IEEE Transactions on Applied Superconductivity,* vol. 31, no. 5, pp. 1-5, 2021.

[28] M. A. P. Sebastian *et al.*, "Study of the Flux Pinning Landscape of YBCO Thin Films With Single and Mixed Phase Additions BaMO3+ Z: M= Hf, Sn, Zr and Z= Y2O3, Y211," *IEEE Transactions on Applied Superconductivity,* vol. 27, no. 4, pp. 1-5, 2017.

[29] S. A. Harrington *et al.*, "Self-assembled, rare earth tantalate pyrochlore nanoparticles for superior flux pinning in YBa(2)Cu(3)O(7-delta) films," *Superconductor Science & Technology,* vol. 22, no. 2, Feb 2009, doi: 10.1088/0953-2048/22/2/022001.

[30] A. Goyal, S.-h. Wee, J. Shin, C. Cantoni, E. Specht, and Y. Zuev, "Engineered Defects in Coated Conductors," in *Materials Science & Technology 2010*, Houston, Oct 2010, pp. 17-22.

[31] H. Tobita *et al.*, "Fabrication of BaHfO3 doped Gd1Ba2Cu3O7-delta coated conductors with the high I-c of 85 A/cm-w under 3 T at liquid nitrogen temperature (77 K)," (in English), *Superconductor*

Science & Technology, vol. 25, no. 6, Jun 2012, doi: 10.1088/0953-2048/25/6/062002.

[32] T. Matsushita *et al.*, "Improvement of flux pinning performance at high magnetic fields in GdBa2Cu3Oy coated conductors with BHO nano-rods through enhancement of B-c2," (in English), *Superconductor Science & Technology,* vol. 25, no. 12, Dec 2012, doi: 10.1088/0953-2048/25/12/125003.

[33] S. Kang *et al.*, "High-performance high-T-c superconducting wires," (in English), *Science,* Article vol. 311, no. 5769, pp. 1911-1914, Mar 2006, doi: 10.1126/science.1124872.

[34] A. Goyal *et al.*, "Irradiation-free, columnar defects comprised of self-assembled nanodots and nanorods resulting in strongly enhanced flux-pinning in YBa2Cu3O7-delta films," *Superconductor Science & Technology,* vol. 18, no. 11, pp. 1533-1538, Nov 2005, doi: 10.1088/0953-2048/18/11/021.

[35] K. Matsumoto *et al.*, "Enhancement of critical current density of YBCO films by introduction of artificial pinning centers due to the distributed nano-scaled Y2O3 islands on substrates," (in English), *Physica C-Superconductivity and Its Applications,* Article; Proceedings Paper vol. 412, pp. 1267-1271, Oct 2004, doi: 10.1016/j.physc.2004.01.157.

[36] T. Haugan, P. N. Barnes, R. Wheeler, F. Meisenkothen, and M. Sumption, "Addition of nanoparticle dispersions to enhance flux pinning of the YBa2Cu3O7-x superconductor," *Nature,* vol. 430, no. 7002, pp. 867-870, Aug 2004, doi: 10.1038/nature02792.

[37] T. Aytug *et al.*, "Enhancement of flux pinning and critical currents in YBa2Cu3O7-delta films by nanoscale iridium pretreatment of substrate surfaces," (in English), *J Appl Phys,* Article vol. 98, no. 11, p. 5, Dec 2005, doi: 10.1063/1.2138370.

[38] J. Gutierrez *et al.*, "Strong isotropic flux pinning in solution-derived YBa2Cu3O7-x nanocomposite superconductor films," (in English), *Nature Materials,* Article vol. 6, no. 5, pp. 367-373, May 2007, doi: 10.1038/nmat1893.

[39] C. V. Varanasi, J. Burke, H. Wang, J. H. Lee, and P. N. Barnes, "Thick YBa(2)Cu(3)O(7-x)+BaSnO(3) films with enhanced critical current density at high magnetic fields," *Applied Physics Letters,* vol. 93, no. 9, Sep 2008, doi: 10.1063/1.2976683.

[40] T. J. Haugan, P. N. Barnes, T. A. Campbell, N. A. Pierce, F. J. Baca, and I. Maartense, "Flux pinning of Y-Ba-Cu-O films doped with BaZrO3 nanoparticles by multilayer and single target methods," (in English), *Ieee Transactions on Applied Superconductivity,* Article; Proceedings Paper vol. 17, no. 2, pp. 3724-3728, Jun 2007, doi: 10.1109/tasc.2007.899342.

[41] Y. Yoshida *et al.*, "High-critical-current-density epitaxial films of SmBa2Cu3O7-x in high fields," (in English), *Japanese Journal of Applied Physics Part 2-Letters & Express Letters,* Article vol. 44, no. 1-7, pp. L129-L132, 2005, doi: 10.1143/jjap.44.l129.

[42] P. N. Barnes *et al.*, "Minute doping with deleterious rare earths in YBa2Cu3O7-delta films for flux pinning enhancements," (in English), *Applied Physics Letters,* Article vol. 89, no. 1, p. 3, Jul 2006, doi: 10.1063/1.2219391.

[43] Y. Yoshida *et al.*, "Controlled nanoparticulate flux pinning structures in RE1+xBa2-xCu3Oy films," (in English), *Physica C-Superconductivity and Its Applications,* Article; Proceedings Paper vol. 445, pp. 637-642, Oct 2006, doi: 10.1016/j.physc.2006.04.059.

[44] T. Matsushita, *Flux Pinning in Superconductors*. Berlin: Springer, 2007.

[45] J. Z. Wu, R. L. S. Emergo, X. Wang, G. Xu, T. J. Haugan, and P. N. Barnes, "Strong nanopore pinning enhances J(c) in YBa(2)Cu(3)O(7-delta) films," (in English), *Applied Physics Letters,* Article vol. 93, no. 6, p. 3, Aug 2008, doi: 10.1063/1.2970965.

[46] V. Selvamanickam, M. H. Gharahcheshmeh, A. Xu, E. Galstyan, L. Delgado, and C. Cantoni, "High critical currents in heavily doped (Gd,Y)Ba2Cu3Ox superconductor tapes," (in English), *Applied Physics Letters,* vol. 106, no. 3, p. 032601, Jan 19 2015, doi: 10.1063/1.4906205.

[47] P. Mele *et al.*, "Systematic study of the BaSnO 3 insertion effect on the properties of YBa 2 Cu 3 O 7− x films prepared by pulsed laser ablation," *Superconductor Science and Technology,* vol. 21, no. 12, p. 125017, 2008. [Online]. Available: http://stacks.iop.org/0953-2048/21/i=12/a=125017.

[48] J. MacManus-Driscoll *et al.*, "Strongly enhanced current densities in superconducting coated conductors of YBa2Cu3O7–x+ BaZrO3," *Nature materials,* vol. 3, no. 7, pp. 439-443, 2004.

[49] J. J. Shi and J. Z. Wu, "Micromechanical model for self-organized secondary phase oxide nanorod arrays in epitaxial YBa2Cu3O7-delta films," *Philosophical Magazine,* vol. 92, no. 23, pp. 2911-2922, 2012, doi: 10.1080/14786435.2012.682173.

[50] P. Pahlke *et al.*, "Reduced J(c) Anisotropy and Enhanced In-Field Performance of Thick BaHfO3-Doped YBa2Cu3O7-delta Films on ABAD-YSZ Templates," (in English), *Ieee Transactions on Applied Superconductivity,* vol. 26, no. 3, Apr 2016, doi: 10.1109/Tasc.2016.2541998.

[51] R. L. S. Emergo, J. Z. Wu, T. J. Haugan, and P. N. Barnes, "Tuning porosity of YBa2Cu3O7-delta vicinal films by insertion of Y2BaCuO5 nanoparticles," (in English), *Applied Physics Letters,* Article vol. 87, no. 23, p. 3, Dec 2005, doi:10.1063/1.2140467.

[52] F. J. Baca, D. Fisher, R. L. S. Emergo, and J. Z. Wu, "Pore formation and increased critical current density in YBa2Cu3Ox films deposited on a substrate surface modulated by Y2O3 nanoparticles," (in English), *Superconductor Science & Technology,* Article vol. 20, no. 6, pp. 554-558, Jun 2007, doi: 10.1088/0953-2048/20/6/011.

[53] P. Mele *et al.*, "High pinning performance of YBa2Cu3O7-x films added with Y2O3 nanoparticulate defects," (in English), *Superconductor*

Science & Technology, vol. 28, no. 2, Feb 2015, doi: 10.1088/0953-2048/28/2/024002.

[54] D. Cherrad, D. Maoucheb, M. Reffas, and A. Benamrania, "Structural, elastic, electronic and optical properties of the cubic perovskites CaXO3 (X = Hf and Sn)," *Solid State Commun.,* vol. 150, 2010.

[55] Z. F. Hou, "Elasticity, electronic structure, and dielectric property of cubic SrHfO3 from first-principles," *Phys. Status Solidi B,* vol. 246, no. 1, pp. 135-139, 2009.

[56] R. Terki, H. Feraoun, G. Bertrand, and H. Aourag, "Full potential calculation of structural, elastic and electronic properties of BaZrO3 and SrZrO3," (in English), *Physica Status Solidi B-Basic Solid State Physics,* vol. 242, no. 5, pp. 1054-1062, Apr 2005, doi: DOI 10.1002/pssb.200402142.

[57] J. J. Shi and J. Z. Wu, "Influence of the lattice strain decay on the diameter of self assembled secondary phase nanorod array in epitaxial films," *J Appl Phys,* vol. 118, no. 16, Oct 2015, Art no. 164301, doi: 10.1063/1.4934640.

[58] J. Z. Wu *et al.*, "The Effect of Lattice Strain On the Diameter of BaZrO3Nanorods in Epitaxial YBa2Cu3O7-d Films," *Superconductor Science & Technology,* vol. 27, p. 044010, 2014.

[59] P. Kuzel, C. Dugautier, and P. Moch, "Comparative study of hypersonic propagation in YBa2Cu3O7-delta single crystals and thin films," (in English), *Journal of Physics-Condensed Matter,* vol. 13, no. 1, pp. 167-175, Jan 8 2001, doi: Doi 10.1088/0953-8984/13/1/317.

[60] M. Lei *et al.*, "Elastic-Constants of a Monocrystal of Superconducting Yba2cu3o7-Delta," (in English), *Phys Rev B,* vol. 47, no. 10, pp. 6154-6156, Mar 1 1993, doi: DOI 10.1103/PhysRevB.47.6154.

[61] H. Yang *et al.*, "Self-assembled multilayers and enhanced superconductivity in (YBa2Cu3O7-x)(0.5): (BaZrO3)(0.5) nanocomposite films," (in English), *J Appl Phys,* vol. 106, no. 9, Nov 1 2009, doi: 10.1063/1.3257238.

[62] J. Z. Wu, J. J. Shi, F. J. Baca, R. Emergo, J. Wilt, and T. J. Haugan, "Controlling BaZrO3 nanostructure orientation in YBa2Cu3O7-delta films for a three-dimensional pinning landscape," *Superconductor Science & Technology,* vol. 28, no. 12, Dec 2015, Art no. 125009, doi: 10.1088/0953-2048/28/12/125009.

[63] F. J. Baca, P. N. Barnes, R. L. S. Emergo, T. J. Haugan, J. N. Reichart, and J. Z. Wu, "Control of BaZrO(3) nanorod alignment in YBa(2)Cu(3)O(7-x) thin films by microstructural modulation," (in English), *Applied Physics Letters,* Article vol. 94, no. 10, p. 3, Mar 2009, doi: 10.1063/1.3097234.

[64] J. F. Baca *et al.*, "Interactive Growth Effects of Rare-Earth Nanoparticles on Nanorod Formation in YBa2Cu3Ox Thin Films," *Advanced Functional Materials,* vol. 23, no. 38, 2013, doi: 10.1002/adfm.201203660.

[65] B. Maiorov *et al.*, "Synergetic combination of different types of defect to optimize pinning landscape using BaZrO3-doped YBa2Cu3O7," *Nature materials,* vol. 8, no. 5, pp. 398-404, 2009, doi: 10.1038/nmat2408.

[66] B. Gautam, Sebastian, M.A., Chen, S.H., Shi, J., Haugan, T., Xing, Z.W., and Wu, J.Z., "Transformational dynamics of BZO and BHO nanorods imposed by Y2O3 nanoparticles for improved isotropic pinning in YBa2Cu3O7 thin films," *AIP Advances* vol. 7, p. 075308, 2017.

[67] C. Cantoni *et al.*, "Strain-driven oxygen deficiency in self-assembled, nanostructured, composite oxide films," *ACS nano,* vol. 5, no. 6, pp. 4783-4789, 2011.

[68] A. K. Jha and K. Matsumoto, "Interfaces in REBCO-Based Nanocomposite Thin Films and their Contribution to Vortex Pinning," in *Surfaces and Interfaces of Metal Oxide Thin Films, Multilayers, Nanoparticles and Nano-composites*: Springer, 2021, pp. 205-221.

[69] J. Wu, B. Gautam, and V. Ogunjimi, "Pinning Efficiency of Artificial Pinning Centers in Superconductor Nanocomposite Films," in *Superconductivity: From Materials Science to Practical Applications*, P. Mele *et al.* Eds. Cham: Springer International Publishing, 2020, pp. 29-52.

[70] B. Gautam *et al.*, "Probing the effect of interface on vortex pinning efficiency of one-dimensional BaZrO3 and BaHfO3 artificial pinning centers in YBa2Cu3O7-x thin films," *Applied Physics Letters,* vol. 113, no. 21, p. 212602, 2018.

[71] G. Blatter, M. V. Feigelman, V. B. Geshkenbein, A. I. Larkin, and V. M. Vinokur, "VORTICES IN HIGH-TEMPERATURE SUPERCONDUCTORS," (in English), *Reviews of Modern Physics,* Review vol. 66, no. 4, pp. 1125-1388, Oct 1994, doi: 10.1103/RevModPhys.66.1125.

[72] V. Ogunjimi *et al.*, "Enhancing magnetic pinning by BaZrO3 nanorods forming coherent interface by strain-directed Ca-doping in YBa2Cu3O7−x nanocomposite films," *Superconductor Science and Technology,* vol. 34, no. 10, p. 104002, 2021/09/07 2021, doi: 10.1088/1361-6668/ac1fd3.

[73] J. Z. Wu *et al.*, "Enabling coherent BaZrO3 nanorods/YBa2Cu3O7− x interface through dynamic lattice enlargement in vertical epitaxy of $BaZrO_3/YBa_2Cu_3O_{7-x}$ nanocomposites," *Superconductor Science and Technology,* vol. 35, no. 3, p. 034001, 2022.

[74] M. Panth *et al.*, "Multilayer $YBa_2Cu_3O_{7-x}/Ca_{0.3}Y_{0.7}Ba_2Cu_3O_{7-x}$ Nanocomposite Films With 2–8% $BaZrO_3$ Doping for High-Field Applications," *IEEE Transactions on Applied Superconductivity,* vol. 32, no. 8, pp. 1-8, 2022.

[75] V. Ogunjimi *et al.*, "Enhancing magnetic pinning by BaZrO3 nanorods forming coherent interface by strain-directed Ca-doping in YBa2Cu3O7− x nanocomposite films," *Superconductor Science and Technology,* vol. 34, no. 10, p. 104002, 2021.

[76] M. Panth *et al.*, "Temperature dependent pinning efficiency in multilayer and single layer BZO/YBCO

nanocomposite films," in *IOP Conference Series: Materials Science and Engineering*, 2022, vol. 1241, no. 1: IOP Publishing, p. 012021.

[77] G. Hammerl *et al.*, "Enhanced supercurrent density in polycrystalline YBa2Cu 3O7-δ at 77 K from calcium doping of grain boundaries," *Nature,* vol. 407, no. 6801, pp. 162-164, 2000.